The influence of electrolyte composition and electrolysis modes on the surface morphology, growth kinetics, phase-structural state, and mechanical properties of MAO coatings on the V95 aluminum alloy (with Zn as the main alloying element) was studied. The possibility of forming a continuous MAO coating on the V95 alloy with a base layer thickness of more than 100 μm and a surface roughness of less than 5 μm was found. The study of the growth kinetics of MAO coatings on the V95 alloy showed that the highest growth rate of the base coating layer (about 0.83 μm/min) occurs in the 1 g/L KOH+6 g/L Na_2SiO_3 electrolyte. Although an increase in the relative content of the silicate component (Na_2SiO_3) provides a fairly high growth rate of the coating, the growth rate of the base layer remains rather low (0.38–0.40 μm/min). This makes the oxidation process in these electrolytes less technological.

The study of the phase-structural state of the base coating layer showed that it has a crystalline structure, in which the main phase is aluminum oxide γ–Al_2O_3 (90–97 %). Crystallites of α-Al_2O_3 and mullite ($3Al_2O_3{\cdot}2SiO_2$) are formed as the second phase. With an increase in process time in electrolytes with the highest relative content of the alkaline component (1 g/L KOH+6 g/L Na_2SiO_3), the relative content of the hardest α-Al_2O_3 phase increases (up to 5 %). The hardness of such coatings with an oxidation time of 180 minutes reaches 14,000 MPa. Thus, the study has shown the advisability of using MAO treatment for the V95 alloy, since it can significantly increase the surface hardness and thereby guarantee its high wear resistance. The combination of high hardness with a relatively high coating growth rate makes it possible to recommend oxidation in the 1 g/L KOH and 6 g/L Na_2SiO_3 electrolyte as the most technologically advanced for improving the mechanical characteristics of the surface of products made of V95 alloy

Keywords: micro-arc oxidation, anode-cathode mode, electrolyte composition, Al–Zn–Mg–Cu, thickness, phase composition, hardness

UDC 539.216.2: 537.52
DOI: 10.15587/1729-4061.2020.217691

IDENTIFICATION OF REGULARITIES OF FORMATION OF THE PHASE-STRUCTURAL STATE AND PROPERTIES OF COATINGS OBTAINED BY MICRO-ARC OXIDATION OF HIGH-STRENGTH V95 ALLOY

V. Subbotina
PhD, Associate Professor*
E-mail: subbotina.valeri@gmail.com
O. Sobol
Doctor of Physical and Mathematical Sciences, Professor*
E-mail: sool@kpi.kharkov.ua
V. Belozerov
PhD, Professor*
E-mail: belozerov.valerii@gmail.com
*Department of Materials Science
National Technical University
"Kharkiv Polytechnic Institute"
Kirpichova str., 2, Kharkiv, Ukraine, 61002

Received date 19.10.2020
Accepted date 01.12.2020
Published date 11.12.2020

1. Introduction

The current trend towards constant updating of technologies in mechanical engineering to increase the competitiveness of products requires the creation of new materials to achieve the required functional properties [1, 2]. In this regard, structural engineering is the most effective method for achieving the required material properties [3, 4]. This method is especially effective for highly non-equilibrium conditions of material formation, when process modeling is not possible due to the multiparametry and uncertainty of the final solutions [5, 6]. Such processes include methods of surface modification by plasma flows [7, 8]. In this case, the modification of the structure and surface properties of materials takes place both in the base material and by forming a new type of material with the required properties on the surface [9, 10]. The first type is the modification of the base material properties through the implantation of modifying elements. In this case, there is a change in the phase-structural state of the base [11, 12]. In this direction, the method of ionic nitriding has received the greatest development [13, 14]. The use of the second type of surface modification provides a qualitatively new phase composition and surface properties. This turned out to be especially effective when new physical and mechanical properties need to be achieved [15, 16]. The use of highly ionized controlled ion-plasma flows made it possible to obtain superhigh mechanical properties for this type of modification. For this, two scientific and practical approaches were used: by optimizing the composition [17] and by creating new types of multilayer composites with nanothick layers [18]. The main problem in the case of creating new materials on the surface is their adhesion to the base material.

In this sense, a universal method of surface modification is the growth of a coating with the required properties

in both directions from the initial surface. This effect can be achieved by modifying the surface by micro-arc oxidation [19, 20], which determines the necessity and urgency of this method.

2. Literature review and problem statement

As shown in [21], during micro-arc oxidation, a spark and an arc appear in the "thinner" places of the dielectric film. In the arc zone (with a temperature of more than 3,000 °C), an oxide is formed, which increases the thickness of the dielectric layer, while the discharge is displaced to the next point, where the dielectric film is thinner [22, 23]. In this case, a characteristic feature of micro-arc discharges is the division of the main current-conducting channel into a multitude of microchannels [24]. These microchannels move continuously over the surface of the oxide layer (i.e., micro-discharges, moving over the entire surface, "heal" weak, porous spots, which contributes to an increase in coating density). Therefore, the elemental composition of the base material is one of the determining factors for the efficiency of such a process [25, 26]. Therefore, the essence of the problem revealed in the analysis of studies [21–26] is the lack of systematic research on the influence of the elemental composition on the features of microplasma processes during oxidation and formation of the phase composition of MAO coatings.

For aluminum-based alloys, process optimization is largely determined by the possibility of forming a phase composition based on the hardest polymorphic modification of aluminum oxide – the α-Al_2O_3 (corundum) phase [27, 28]. However, there are currently no special phase-structural studies of stabilization conditions for the α-Al_2O_3 phase at different contents of alloying elements. Although there are a number of studies that provide some experimental results in this direction. Thus, in [29, 30], it was found that the use of Mg and Cu as alloying elements promotes uniform growth of the coating and stimulates the $\gamma \rightarrow \alpha$ polymorphic transformation in it. On the contrary, the use of Zn as an alloying element complicates the course of the micro-arc oxidation process [31] and requires additional research to develop a technology that ensures the oxidation process in the micro-arc discharge mode. However, a significant part of aluminum alloys used today, requiring an increase in surface properties, belong to the Al-Zn-Mg-Cu system [32, 33]. The reason for the demand for this type of alloys is high ultimate tensile strength (600–700 MPa) and yield stress close to it [34]. This is achieved by a complex alloying with zinc, magnesium and copper, which form solid solutions and various metal compounds with aluminum and among themselves – $MgZn_2$, S (Al_2CuMg), T ($Mg_4Zn_3Al_3$). Only such a complex alloying and formation of hardening compounds provide significant hardening during heat treatment of this alloy.

In the Ukrainian industry, the most used alloy of the Al-Zn-Mg-Cu system is high-strength V95 alloy (GOST 4784-97, American analogue – 7075 alloy, European standard (EN) ENAW-7075 ENAW-AlZn5.5MgCu). The reason is that it is the strongest aluminum alloy currently used in the industry. The alloy is used for highly loaded structures operating under high compressive pressure, since it has the highest tensile strength of all known aluminum alloys. Due to such unique operational characteristics, which are not inferior to the properties of steel, it is currently one of the main structural materials used in aviation and nuclear technology [35, 36]. However, alloys of the Al-Zn-Mg-Cu system are characterized by such disadvantages as increased corrosion sensitivity and cracking under the action of sharp cuts, scratches and distortions [37]. To solve these problems, the obligatory plasma oxidation of the surface is used. However, as shown in the review [31], at present there is no unified approach for optimizing the plasma oxidation modes of multielement alloys. And basically empirical selection of modes is used to optimize functional characteristics, which is a very time-consuming and, moreover, not always effective process. This is due to the fact that research is mainly aimed at achieving certain properties necessary for solving specific industrial problems, and there are no generalized optimization criteria for these cases. In this regard, the study suggests using the phase-structural state as such a basic criterion for comparison and optimization. This makes it possible to unify the comparative base for different types of aluminum alloys by determining the percentage of basic γ-Al_2O_3 and α-Al_2O_3 phases (as well as mullite as an accompanying phase during electrolysis in an alkali silicate electrolyte) as the main comparison indicator. As additional physical and technological criteria (necessary for industrial use), it is proposed to use the growth kinetics of the coating and the morphology of the surface formed, and hardness measurement as a criterion for optimizing mechanical properties.

3. The aim and objectives of the study

The aim was to reveal the regularities of the influence of the electrolyte composition and electrolysis modes of the Al-Zn-Mg-Cu system alloy on the basic (phase-structural state) and physico-technological (growth kinetics, surface morphology) generalized comparison criteria for MAO coatings based on aluminum alloys, and also a criterion for optimizing mechanical properties (hardness).

To achieve the aim, the following objectives were set:

– to study the effect of electrolyte composition and electrolysis conditions on the morphology of the growth surface of MAO coatings formed on the V95 aluminum alloy (Al-Zn-Mg-Cu multielement system);

– to determine the growth kinetics of coatings and changes in sample size depending on the composition of the alkali-silicate electrolyte;

– to determine the regularities of the formation of the phase composition of coatings on the V95 alloy for different compositions of the alkali-silicate electrolyte and to study the effect of electrolysis conditions on the hardness of MAO coatings.

4. Materials and methods for studying the effect of electrolysis conditions on the structure and properties of MAO coatings

The study was carried out on deformed V95 aluminum alloys (the Al–Zn–Mg–Cu system, foreign analogues: ENAW-7075 (European Union), 7075 (USA)). The chemical composition of the alloy is given in Table 1.

Table 1

Chemical composition of V95 alloy

Basic components				Impurities		
Mg	Mn	Cu	Zn	Cr	Ni	Fe
1.8–2.8	0.2–0.6	1.4–2.0	5.0–7.0	0.10–0.25	0.1	0.5

This alloy composition is due to the fact that the amount of alloying elements in it, as hardened by heat treatment, must be higher than the limit of their solubility in aluminum at operating temperature.

Micro-arc oxidation was carried out in a 100 liter bath. During the MAO process, cooling and bubbling of the electrolyte were provided. The average voltage was 380 V.

As is known, the uniqueness of the micro-arc oxidation process is that the growth of the oxide layer occurs both deep into the material (by oxygen diffusion and plasma reaction) and partly with an increase in thickness on the surface [31, 38]. In this case, the base layer, consisting of dense solid modifications of oxides, is formed mainly as an internal layer (with a slight increase on the surface due to the difference between the specific volumes of the metal and oxide phases). Due to the high plasma density and high temperature in the micro-arc breakdown channels during the oxidation of aluminum alloys, the base layer mainly consists of the hardest α-Al_2O_3 and γ–Al_2O_3 phases [31, 38]. The growth of the outer layer occurs at lower compression, lower plasma density and process temperature, and therefore is carried out due to the formation of less heat-resistant and less solid oxide phases, for example, mullite [27, 30, 38].

For industrial use, the removal of the technological layer is required, since it consists of low-hardness phases, has a high porosity and low wear resistance. The technological layer is removed by stripping on abrasive paper [38].

It should be noted that a significant amount of zinc (5–7 %) is present in the V95 alloy, which impairs the oxidation ability of the alloy. Therefore, it was necessary to conduct primary studies to select micro-arc oxidation conditions, which ensured uniformity of the coating during the MAO process. For this, the electrolyte composition was varied in the study. The most effective electrolyte components were used: alkali (KOH) and silicate component (Na_2SiO_3).

Based on the analysis of the results for different oxidation modes [27, 30, 39, 40], three modes were chosen as suitable for obtaining homogeneous coatings for further studies:

1) electrolyte composition 1:6 (1 g/L KOH and 6 g/L Na_2SiO_3), current density j=20 A/dm^2, τ=180 min, electrolyte temperature t=20 °C;

2) electrolyte composition 2:12 (2 g/L KOH and 12 g/L Na_2SiO_3), j=20 A/dm^2, τ=180 min, t=20 °C;

3) electrolyte composition 0.7:8 (0.7 g/L KOH and 8 g/L Na_2SiO_3), j=60 A/dm^2, τ=180 min, t=60 °C;

Note that in the electrolyte of the third composition, a homogeneous continuous coating was achieved only at a fairly high temperature t=60 °C, which makes this mode less technological. However, in order to create the scientific foundations of the phase-structural engineering of multi-element aluminum alloys, such studies are expedient.

Also, MAO coatings formed in the 1:12 (1 g/L KOH and 12 g/L Na_2SiO_3) and 2:6 (2 g/L KOH and 6 g/L Na_2SiO_3) electrolytes, in which the micro-arc oxidation process was unstable (microarc passed into arc), were used for comparison.

Determination of the phase composition of MAO coatings was carried out according to the results of X-ray phase analysis. The studies were carried out on a DRON-3 setup (Burevestnik, Russia) in monochromatic K_α–Cu radiation. Diffraction spectra were recorded using the Bragg-Brentano reflection scheme [41]. The survey was carried out both in continuous and pointwise mode with a step of 2θ=0.1°. The minimum detectability of structural components is about 1 vol. %.

For quantitative phase analysis, the method of reference mixtures was used [42]. For this, calibration graphs of the dependence of the comparison line intensity on mixture composition were constructed. α-Al_2O_3 (ASTM Card File 10-173), γ–Al_2O_3 (ASTM Card File 10-425) and mullite (γ–Al_2O_3, ASTM Card File 15-776) were used as the basic components of the coating composition. If peaks from the aluminum substrate appeared in the diffraction spectra, they were not taken into account when calculating the coating composition.

The coating thickness was determined using a VT-10 NTs vortex thickness gauge (Kontrolpribor, Russia). The error in measuring the coating thickness is no more than 5 % at the smallest coating thickness (about 10 μm). With a larger coating thickness, the accuracy of thickness measurement increases (for example, at a thickness of 50 μm, the measurement error is no more than 2 %).

The study of the surface morphology and side section of the coatings was carried out by the method of scanning electron microscopy on REMMA 101 (JSC SELMI, Ukraine). To analyze the surface roughness, a topographic contrast was used, based on the fact that electron reflection and secondary electron emission depend on the angle of beam incidence on the sample. The angle of incidence changes due to the sample roughness (topography), resulting in the formation of contrast associated with the shape of the object.

The microhardness was determined using a PMT-3 device (AO LOMO, Russia).

5. Results of studying the effect of electrolysis modes on surface morphology, growth kinetics, phase composition and hardness of MAO coatings

5. 1. Influence of electrolyte composition and electrolysis conditions on the surface morphology of MAO coatings on the V95 alloy

Scanning electron microscopy was used to study the surface morphology. The quality of MAO coatings is most clearly manifested after the removal of the technological layer. In this case, MAO coatings formed in the 2 g/L KOH+12 g/L Na_2SiO_3 electrolyte have the most homogeneous structure of the base layer.

At the same time, the base layer formed in the 2 g/L KOH+6 g/L Na_2SiO_3 (Fig. 1, *a*) electrolyte, and especially when formed in the 1 g/L KOH+12 g/L Na_2SiO_3 electrolyte (Fig. 1, *b*), consists of discontinuities and large through pores (shown by the white arrows in Fig. 1, *a*, *b*). This surface morphology of the base layer is determined by the peculiarities of micro-arc oxidation [31]. Upon visual observation of the oxidation process in various electrolytes, it was found that for all electrolytes there is a stage of sparking, microarc and arc discharges, but the duration of this stage is different for different electrolytes.

In the electrolytes with the homogeneous coating, the duration of the micro-arc discharge stage is long-term. All discharges have the same glow. With an increasing coating thickness, the glow intensity, as well as the number of micro-discharges decreases. In this case, the coating is homogeneous with low porosity.

Formation of a defective coating on the V95 alloy, upon reaching a certain thickness (about 50 μm, which is less than necessary for practical use (more than 100 μm)), leads to discharges. These discharges are visually recorded as a single

powerful glow, which is characteristic of arc discharges [31]. The power of such arcs is sufficient for heating the substrate, melting the coating, and forming craters, as can be seen in Fig. 1, *a*, *b*.

In addition to studying the surface morphology of the MAO coating, its structure was also studied on cross sections. The image of cross sections is shown in Fig. 2. It is known [31] that one of the microstructural features of oxide coatings formed in the anode-cathode mode of micro-arc oxidation is their two-layer structure, which is also manifested during the oxidation of the V95 alloy.

The top layer of the coating (loose with a highly developed surface, making it not wear-resistant) is easily removed by sanding on abrasive paper.

As seen from Fig. 2, the view of the metal-oxide interface (absence of pores, inclusions, exfoliations) indicates good adhesion to the base material.

The technological layer is heterogeneous (with large build-ups formed) even with a fairly uniform morphology of the base layer. SEM images of the technological and base layers formed in the 2 g/L KOH+12 g/L Na_2SiO electrolyte, for which a continuous base coating is provided, are shown in Fig. 3, *a*, *b*. As seen from Fig. 3, the surface of the technological layer of coatings has a sufficiently large heterogeneity with the build-ups (shown in Fig. 3, *a* by arrows), reaching 30 μm (Fig. 3, *c*). After removing the technological layer, the surface morphology becomes homogeneous (Fig. 3, *b*), and the surface roughness does not exceed 5 μm (Fig. 3, *d*).

Even with a relatively small change in the electrolyte composition by increasing the content of the silicate component (electrolyte composition 1 g/L KOH and 12 g/L Na_2SiO_3), the morphology of the coating remains highly heterogeneous even after the removal of the technological layer.

The electron microscopic image of the surface morphology and the profilogram of the MAO coating surface obtained in the 1 g/L KOH and 12 g/L Na_2SiO_3 electrolyte after removing the technological layer are shown in Fig. 4. It can be seen that, in this case, through breakdowns (indicated by white arrows) are observed in the base layer, which are formed, apparently, during the transition from micro-arc to arc oxidation.

Thus, coatings with uniform morphology and low roughness can be obtained by careful selection of the electrolyte during oxidation with no transition from the micro-arc mode to the arc mode.

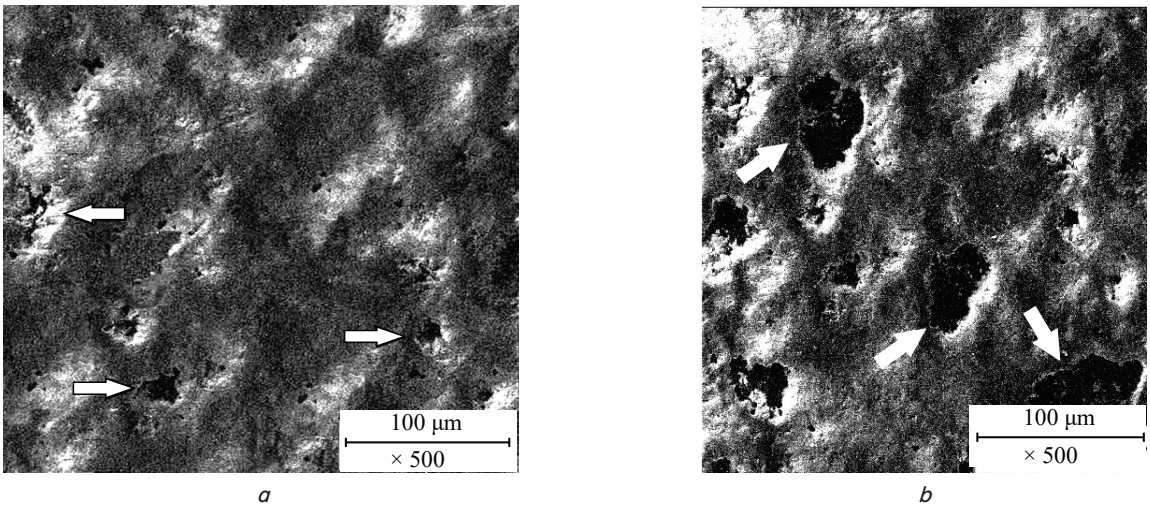

a *b*

Fig. 1. Surface morphology of the base layer of MAO coatings formed during oxidation for 3 hours in the electrolyte: *a* – 2 g/L KOH and 6 g/L Na_2SiO_3; *b* – 1 g/L KOH and 12 g/L Na_2SiO_3

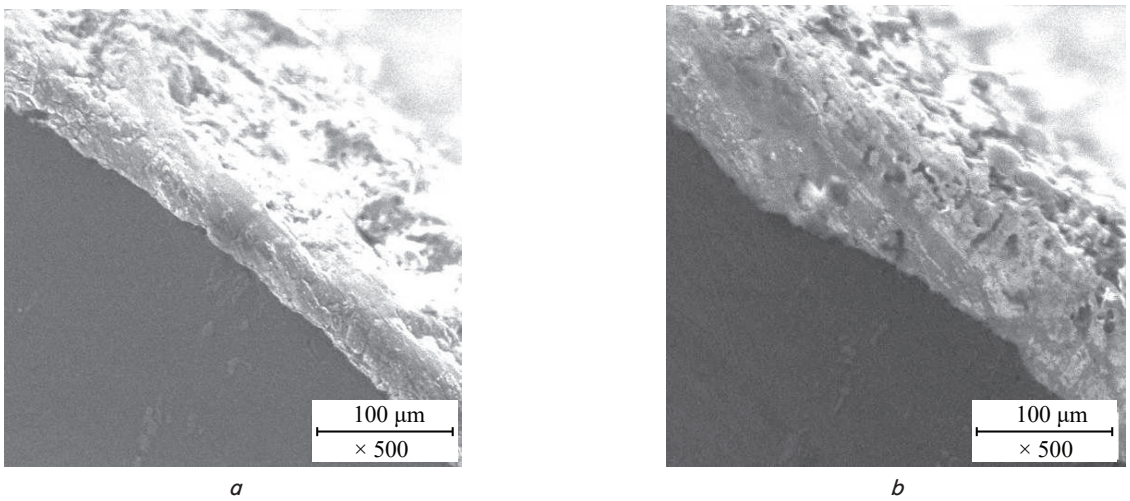

a *b*

Fig. 2. Cross section of MAO coatings formed during oxidation of the V95 alloy in the 1 g/L KOH and 6 g/L Na_2SiO_3 electrolyte for: *a* – 60 min; *b* – 180 min

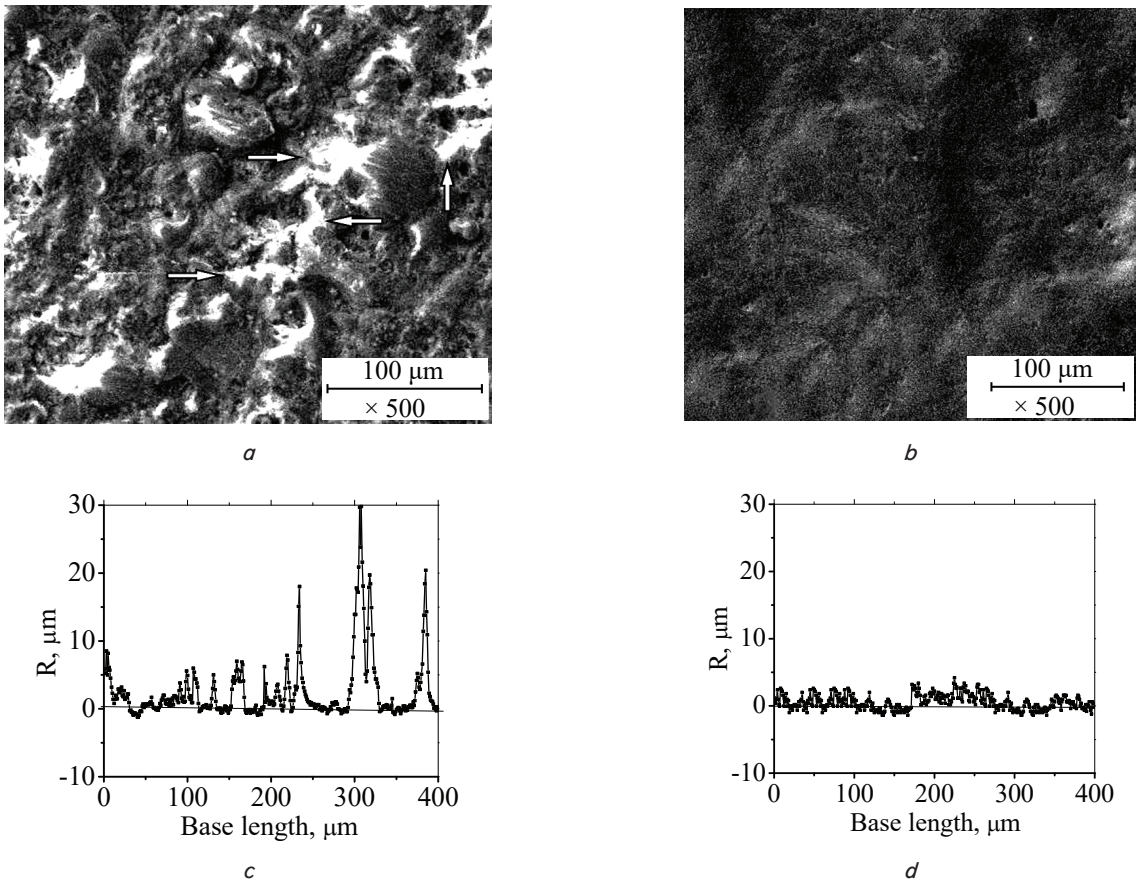

Fig. 3. MAO coating formed in the 1 g/L KOH and 6 g/L Na_2SiO_3 electrolyte, τ=180 min: *a* — scanning electron microscopic image of surface morphology (with the technological layer); *b* — scanning electron microscopic image of surface morphology (after removing the technological layer); *c* — profilogram of surface roughness (with the technological layer); *d* — profilogram of surface roughness (after removing the technological layer)

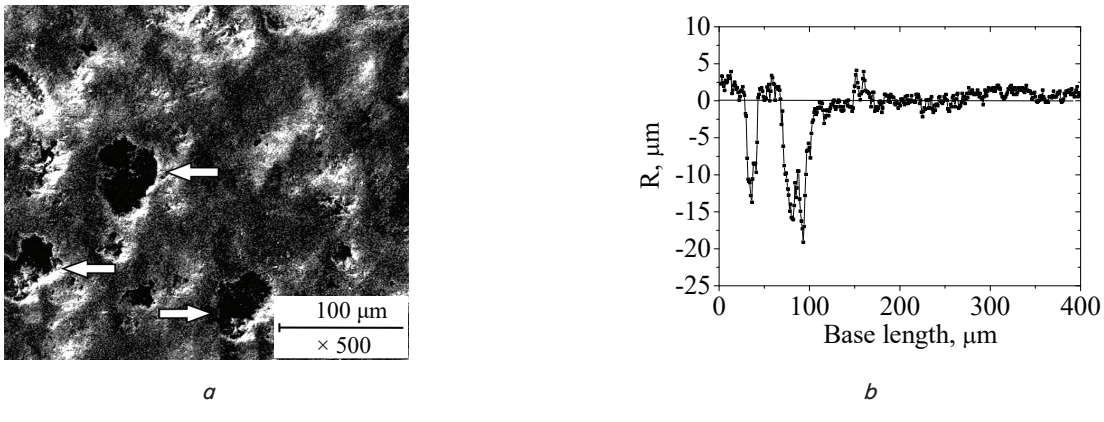

Fig. 4. MAO coating formed in the 1 g/L KOH and 12 g/L Na_2SiO_3 electrolyte, τ=180 min: *a* — scanning electron microscopic image of surface morphology; *b* — profilogram of surface roughness

5. 2. Determination of the growth kinetics of MAO coatings and changes in the V95 alloy sample size in various electrolytes

An important technological parameter of MAO coatings is thickness. In addition, due to the peculiarities of the MAO process, resulting in the coating growth in both directions from the initial surface, an important parameter is the change in the sample size from the initial surface level. The importance of these parameters for the V95 alloy is determined by its use as elements of friction pairs and other precision parts.

The time dependences of the thickness of MAO coatings for different types of electrolytes are shown in Fig. 5 (the thickness value was determined from 4 measurements. The spread in thickness values for most measurements did not exceed 5 μm. With the scale used in Fig. 5, this led in some cases to merging of points with the formation of the area of the obtained coating thickness values for each oxidation time).

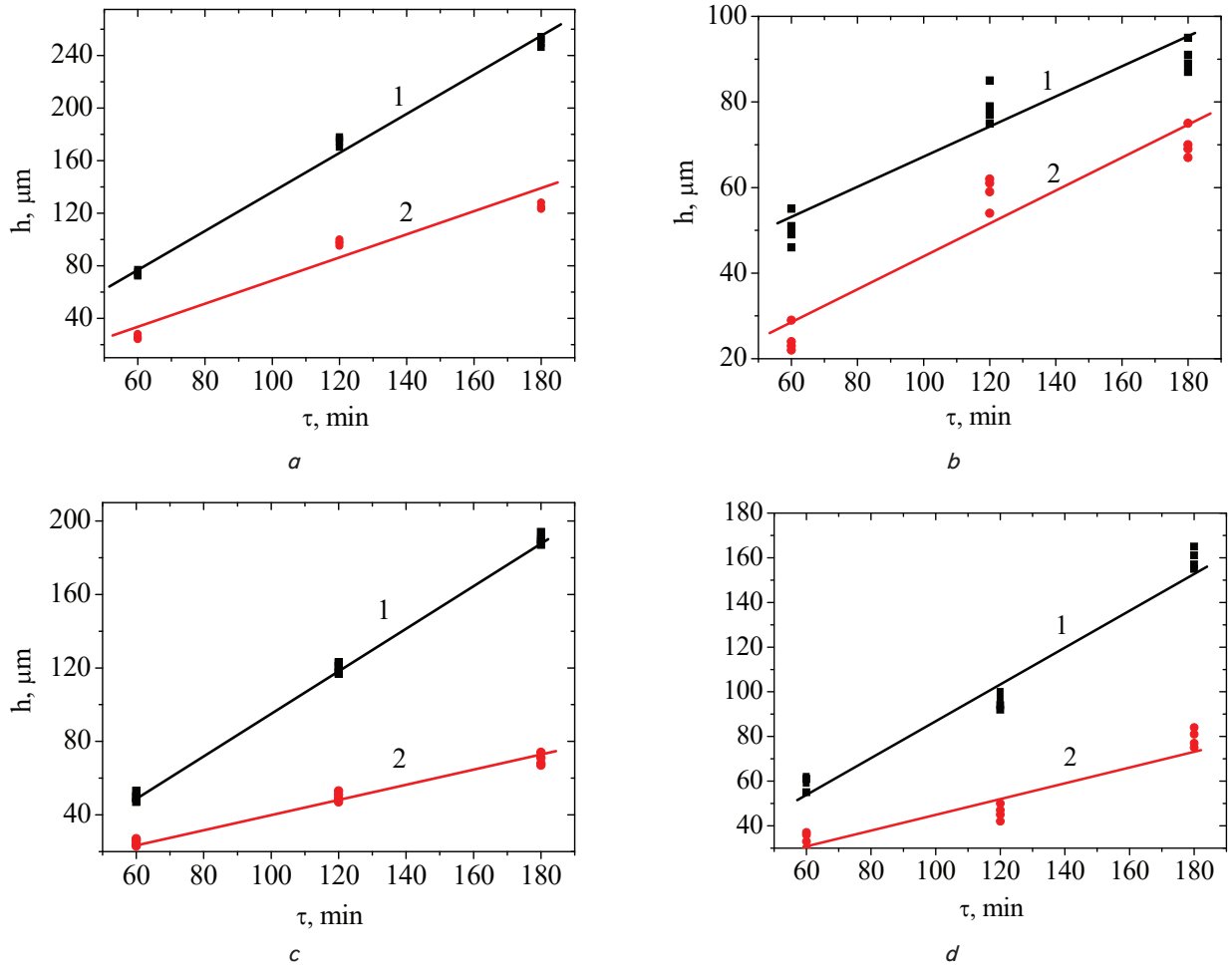

Fig. 5. Dependence of the thickness of MAO coatings (h) on the duration of oxidation in electrolytes (τ) of the following compositions: *a* – 1 g/L KOH+6 g/L Na_2SiO_3 (1 – total coating thickness, 2 – working (base) layer thickness); *b* – 2 g/L KOH+6 g/L Na_2SiO_3 (1 – total coating thickness, 2 – working (base) layer thickness); *c* – 2 g/L KOH+12 g/L Na_2SiO_3 (1 – total coating thickness, 2 – working (base) layer thickness); *d* – 0.7 g/L KOH+8 g/L Na_2SiO_3 (1 – total coating thickness, 2 – working (base) layer thickness)

It can be seen that the experimental points shown in Fig. 5 can be approximated by linear functions, and the coating growth rate can be estimated from the ratio h/τ on the linearized section. This estimate has an error, but can be used for comparison. Thus, determined from the h/τ ratio on the linearized section in Fig. 5, *a*, the growth rate of the coatings formed in the 1 g/L KOH+6 g/L Na_2SiO_3 electrolyte for the total layer thickness is V≈1.46 μm/min. For the working layer, the growth rate is V≈0.83 μm/min. For the coatings formed in the 2 g/L KOH+6 g/L Na_2SiO_3 electrolyte, V varies from 0.33 μm/min for the total layer thickness to 0.37 μm/min for the working coating layer. For the coatings formed in the 2 g/L KOH+12 g/L Na_2SiO_3 electrolyte, V varies from 1.17 μm/min for the total layer thickness to 0.40 μm/min for the working coating layer. The rate of increase in the total thickness (V≈0.83 μm/min) for the coatings formed in the 0.7 g/L KOH+8 g/L Na_2SiO_3 electrolyte is somewhat lower, while the rate of increase in the thickness for the working layer decreased to a lesser extent, V≈0.38 μm/min.

Thus, the highest growth rate of the MAO coating on the V95 alloy is achieved in the 1 g/L KOH+6 g/L Na_2SiO_3 electrolyte, in which the ratio between the silicate and alkaline components is 6:1. A relatively high growth rate of the coating in the 2 g/L KOH+12 g/L Na_2SiO_3 (Fig. 5, *c*) and 0.7 g/L KOH+8 g/L Na_2SiO_3 (Fig. 5, *d*) electrolytes is mainly due to the growth of the technological layer. The growth rate of the base layer in these electrolytes remains low (0.38–0.40 μm/min).

As shown by measurements of the sample sizes before and after oxidation, after the removal of the technological layer, the increase in the sample thickness does not exceed 10 μm (for all types of electrolytes studied) with the longest oxidation time of 3 hours. The change in thickness is associated with an increase in the specific volume of the material during the transition from the metal base to the oxide coating. However, the small value of such a change (less than 10 μm) makes it possible to follow the technical documentation of parts for the tolerance associated with the MAO coating.

5. 3. Regularities of formation of phase composition and hardness of MAO-coatings obtained in various electrolytes

Volume changes in MAO coatings are determined by the type of oxide phases they contain.

The phase composition of MAO coatings was studied by X-ray diffractometry. The XRD pattern of the MAO coating on the V95 alloy, typical for the studies performed in this work, is shown in Fig. 6.

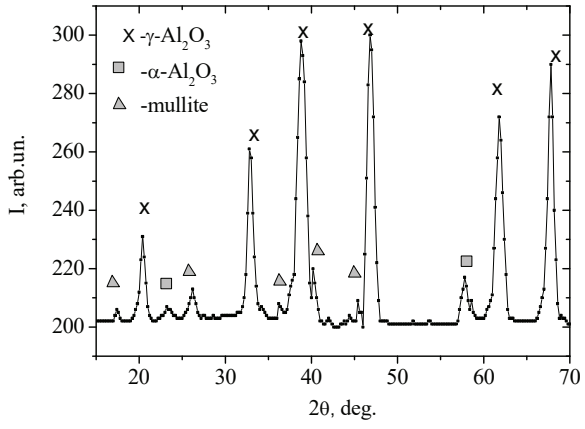

Fig. 6. Section of the X-ray diffraction spectrum of the MAO coating on the V95 alloy obtained in the 1 g/L KOH+6 g/L Na_2SiO_3 electrolyte (τ=120 min.)

Analysis of the obtained diffraction spectra shows that the coatings have a crystalline structure, and the phase composition of the coatings contains three types of aluminum oxides: γ-Al_2O_3, α-Al_2O_3 and mullite ($3Al_2O_3{\cdot}2SiO_2$).

From the data presented in Fig. 7, it can be seen that γ-Al_2O_3 is the main phase in MAO coatings for all types of electrolytes. The highest content of α-Al_2O_3 was found in the coating formed within 180 minutes in the 1 g/L KOH+6 g/L Na_2SiO_3 electrolyte (Fig. 7, *a*). An increase in the relative content of liquid glass (Na_2SiO_3) in the electrolyte stimulates the formation of the mullite phase.

As is known [30, 31], the hardness and wear resistance of the MAO coating depend on phase composition. Of the phases identified in the coating, the α-Al_2O_3 phase has the highest hardness (up to 25,000 MPa), and the lowest hardness (up to 10,000 MPa) is inherent in the mullite phase. Given the fact that the main phase of MAO coatings on the V95 alloy is γ–Al_2O_3, it can be expected that the hardness of the coatings should be close to the hardness of 14,000 MPa characteristic of this phase.

Fig. 8, 9 show the values of hardness measurements depending on the process time (Fig. 8) and coating thickness (Fig. 9). In this case, the hardness was determined by at least 3 measurements.

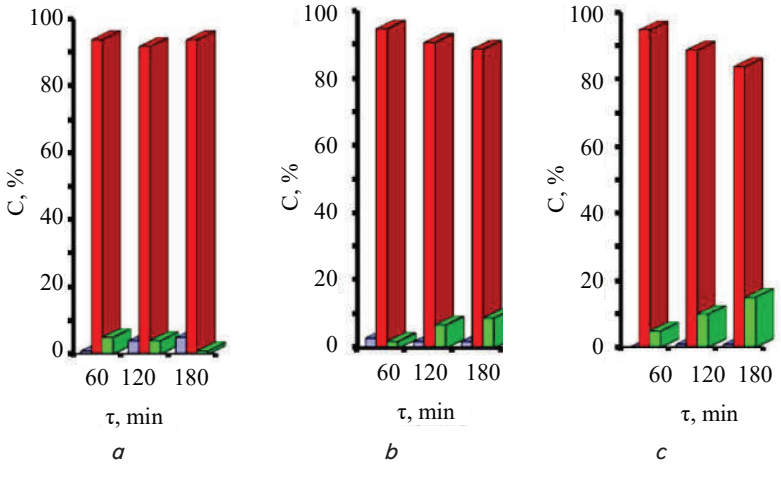

Fig. 7. Influence of electrolyte type and oxidation time on the phase composition of MAO coatings on the V95 alloy: *a* – 1 g/l KOH+6 g/L Na_2SiO_3 electrolyte; *b* – 2 g/L KOH+12 g/L Na_2SiO_3 electrolyte; *c* – 0.7 g/L KOH+8 g/L Na_2SiO_3 electrolyte; – α–Al_2O_3; – γ-Al_2O_3; – $3Al_2O_3{\cdot}2SiO_2$

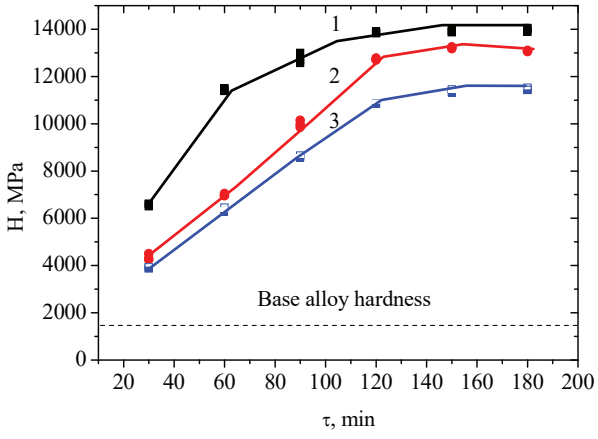

Fig. 8. Dependences of the hardness of MAO coatings on process time: 1 – 1 g/L KOH+6 g/L Na_2SiO_3 electrolyte; 2 – 2 g/L KOH+12 g/L Na_2SiO_3 electrolyte; 3 – 0.7 g/L KOH+8 g/L Na_2SiO_3 electrolyte

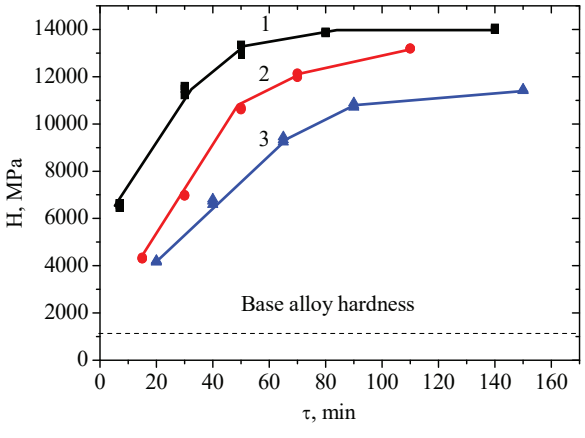

Fig. 9. Dependences of the hardness of MAO coatings on coating thickness: 1 – 1 g/L KOH+6 g/L Na_2SiO_3 electrolyte; 2 – 2 g/L KOH+12 g/L Na_2SiO_3 electrolyte; 3 – 0.7 g/L KOH+8 g/L Na_2SiO_3 electrolyte

Fig. 8, 9 show that hardness dependencies on the deposition time and thickness of the MAO coating have a similar form. This indicates the decisive influence of processes simultaneously caused by changes in the process time and thickness. Such processes during micro-arc oxidation include an increase in discharge power. This results in the temperature increase in the region of the dielectric film breakdown and formation of the α-Al_2O_3 oxide phase. The higher hardness of the coatings formed in the 1 g/L KOH+6 g/L Na_2SiO_3 electrolyte can be explained by the high content of the α-Al_2O_3 phase (Fig. 7), as well as by the ordering of Al^{3+} ions and alloying metals in octahedral and tetrahedral positions [30].

6. Discussion of the results of the electrolysis conditions effect on surface morphology, phase composition and hardness of MAO coatings

Analysis of the topography of the coating surface using scanning electron microscopy

showed (Fig. 1, 3, 4) that the formed technological layer has a branched surface with a high content of discontinuities. As is known [38, 43], during the formation of a coating in alkali-silicate electrolytes on aluminum, this layer mainly consists of a mullite phase with large (up to 70 %) porosity. Large porosity can be a consequence of the intense evolution of hydrogen gas due to water decomposition, and the absorption of these gases by the melt, which is carried to the surface and dissolved, forming surface pores [31].

As shown by X-ray diffraction studies, γ–Al_2O_3 is the main phase in the base MAO coating on the V95 alloy. The hardness characteristic of this phase is 14,000 MPa, which determines the attainable hardness with values close to 14,000 MPa in the MAO coating. In this case, by choosing the electrolyte composition, it is possible to obtain continuous coatings with a low (less than 5 μm) surface roughness (Fig. 3). At the same time, a change only in the relative content of the components in the electrolyte (with the same composition) leads to breakdown and appearance of discontinuities in the base layer (Fig. 4). As a result, its performance is lost. The reason for this is the transition from the micro-arc to the arc mode of the plasma process during the formation of the oxide layer. In general, conditions for the occurrence of arc discharges are associated with several factors: temperature, applied potential difference, thermal conductivity, structure of the oxidized material, electrical resistance of electrolytes and their scattering ability [31]. The instability of micro-arc discharges is based on the fact that the thermal pulse from the discharge does not have time to quickly dissipate. This is the reason for the low speed of movement of micro-arc discharges on the surface of the oxide film and their transition into an arc. For the most technologically advanced electrolysis conditions (at a low temperature, about 20 °C), a stable micro-arc mode for a long (180 minutes) time was provided by electrolytes of two compositions: 1 g/L KOH+6 g/L Na_2SiO_3 and 2 g/L KOH+12 g/L Na_2SiO_3. This made it possible to form an oxide coating on the V95 alloy with a thickness of more than 140 μm and high hardness.

In this regard, it should be noted that, despite the practically identical phase composition (γ–Al_2O_3 content is 94–97 %), the hardness of the coatings changes significantly depending on the MAO process time and thickness (Fig. 8). This is because the structure of γ–Al_2O_3 belongs to the defect type spinel structure with a lack of metal ions. In the spinel structure ($Me^{2+}Me_2^{3+}O_4$), the unit cell includes 32 O^{2-} anions, forming the densest cubic packing with 64 tetrahedral (cations occupy 8) and 32 octahedral (cations occupy 16) voids. Such voids should contain 24 metal ions [44]. The unit cell of γ–Al_2O_3 contains 32 oxygen ions (i.e., the anionic part corresponds to the filling for classical spinel), but the cationic part accounts for 21 1/3 metal ions (i.e. contains 8 $A1_2O_3$ molecules). This is due to the fact that in γ–Al_2O_3, the Al^{3+} ion plays the role of both Me^{2+} and Me^{3+} cations [45]. Al^{3+} ions are statistically distributed over 8 tetrahedral and 16 octahedral positions. Therefore, the structure of γ–Al_2O_3 is called a defect-type spinel structure, and upon exposure to temperature, redistribution of Al^{3+} ions over octahedral and tetrahedral positions can occur, which affects the lattice period and properties [39, 40]. Such a crystal lattice is unstable and its existence requires stabilizers in the form of ions of different elements. In this regard, with a change in the coating thickness (with an increase in oxidation time), the power of the micro-arcs and, accordingly, different conditions for the formation of the γ-phase also change, which is reflected in its structure. Different degrees of alloying of the γ–Al_2O_3 structure with other metals and different temperatures of formation determine the difference in the γ–Al_2O_3 phase hardness. This manifests itself in the formation of coatings in alkali-silicate electrolytes with different ratios of components (KOH and Na_2SiO_3) at different coating thicknesses [31].

However, as it was found in the study, with the optimized formation parameters of MAO coatings, it is possible to increase the surface hardness of the V95 alloy almost 10 times. Such an increase in hardness and associated wear resistance creates good prospects for using this technology to improve performance in friction pairs. However, such use is associated with some difficulties and, first of all, with the need for a number of products made of this alloy to operate in aggressive environments. Such products, for example, include pump parts operating in different (including aggressive) environments. Therefore, studies related to the assessment of protective properties of such coatings against aggressive media are relevant and promising, which is the direction for further continuation of this study.

7. Conclusions

1. The possibility of forming a continuous MAO coating on the V95 alloy with a base layer thickness of more than 100 μm and surface roughness of less than 5 μm was found. This type of coatings is formed in alkali-silicate electrolytes at a low temperature t=20 °C and a KOH/Na_2SiO_3 ratio close to 1:6, when a stable stage of micro-arc discharges is observed during oxidation. In this case, the growth of the base oxide layer occurs mainly deep into the sample, leading to changes in its size after 3-hour oxidation not exceeding 10 μm.

An increase in the relative content of the silicate (Na_2SiO_3) component in the electrolyte leads to a loss of stability of micro-arc discharges and transition to the arc discharge stage. This leads to the appearance of 30–40 μm through discontinuities on the growing coating.

2. The study of the growth kinetics of MAO coatings on the V95 alloy showed that the highest growth rate of the base coating layer of 0.92 μm/min occurs in the 1 g/L KOH+6 g/L Na_2SiO_3 electrolyte. Although an increase in the relative content of the silicate component (Na_2SiO_3) provides a fairly high growth rate of the coating, the growth rate of the base layer remains rather low (0.38–0.40 μm/min). This makes the oxidation process in these electrolytes less technological.

3. The study of the phase-structural state of the base layer of the coating showed that it has a crystalline structure in which the main phase is γ-Al_2O_3 aluminum oxide (90–97 %). Crystallites of α-Al_2O_3 and mullite ($3Al_2O_3{\cdot}2SiO_2$) are formed as the second phase. With an increase in process time (and the associated coating thickness) in the electrolytes with the highest content of the silicate component, an increase in the relative content of the mullite phase ($3Al_2O_3{\cdot}2SiO_2$) occurs. In the electrolytes with the highest relative content of the alkaline component (1 g/L KOH+6 g/L Na_2SiO_3), with an increase in process time, the relative content of the hardest α-Al_2O_3 phase increases (up to 5 %). The hardness of such coatings with an oxidation time of 180 minutes reaches 14,000 MPa.

Acknowledgments

The authors would like to express their gratitude to the Ministry of Education and Science of Ukraine for financial support within the framework of the projects "Development of materials science bases for using high-performance ion-plasma technologies for three-level surface engineering" (state registration number No. 0118U002044) and "Development of materials science bases for structural engineering of Cu and Al-based pseudoalloys" (state registration number No. 0119U002567).

References

1. Hlushkova, D. B., Ryzhkov, Y. V., Kostina, L. L., Demchenko, S. V. (2018). Increase of wear resistance of the critical parts of hydraulic hammer by means of ion-plasma treatment. Problems of Atomic Science and Technology, 1 (113), 208–211.
2. Fedirko, V. M., Pohrelyuk, I. M., Luk'yanenko, O. H., Lavrys', S. M., Kindrachuk, M. V., Dukhota, O. I. et. al. (2018). Thermodiffusion Saturation of the Surface of VT22 Titanium Alloy from a Controlled Oxygen–Nitrogen-Containing Atmosphere in the Stage of Aging. Materials Science, 53 (5), 691–701. doi: https://doi.org/10.1007/s11003-018-0125-z
3. Sobol, O. V., Postelnyk, A. A., Meylekhov, A. A., Andreev, A. A., Stolbovoy, V. A., Gorban, V. F. (2017). Structural Engineering of the Multilayer Vacuum Arc Nitride Coatings Based on Ti, Cr, Mo and Zr. Journal of Nano- and Electronic Physics, 9 (3), 03003-1–03003-6. doi: https://doi.org/10.21272/jnep.9(3).03003
4. Glushchenko, M. A., Belozyorov, V. V., Sobol, O. V., Subbotina, V. V., Zelenskaya, G. I. (2017). Effect of Tantalum on the Texture of Copper Vacuum Condensates. Journal of Nano- and Electronic Physics, 9 (2), 02015-1–02015-5. doi: https://doi.org/10.21272/jnep.9(2).02015
5. Mayrhofer, P. H., Mitterer, C., Hultman, L., Clemens, H. (2006). Microstructural design of hard coatings. Progress in Materials Science, 51 (8), 1032–1114. doi: https://doi.org/10.1016/j.pmatsci.2006.02.002
6. Sobol, O. V., Andreev, A. A., Gorban, V. F., Meylekhov, A. A., Postelnyk, H. O., Stolbovoy, V. A. (2016). Structural engineering of the vacuum Arc ZrN/CrN multilayer coatings. Journal of nano- and electronic physics, 8 (1), 01042-1–01042-5. doi: https://doi.org/10.21272/jnep.8(1).01042
7. Rocha, R. C., Galdino, A. G. de S., Silva, S. N. da, Machado, M. L. P. (2018). Surface, microstructural, and adhesion strength investigations of a bioactive hydroxyapatite-titanium oxide ceramic coating applied to Ti-6Al-4V alloys by plasma thermal spraying. Materials Research, 21 (4). doi: https://doi.org/10.1590/1980-5373-mr-2017-1144
8. Bekkara, M. F., Dascalescu, L., Benmimoun, Y., Zeghloul, T., Tilmatine, A., Zouzou, N. (2018). Modification of surface characteristic and tribo-electric properties of polymers by DBD plasma in atmospheric air. The European Physical Journal Applied Physics, 81 (1), 10801. doi: https://doi.org/10.1051/epjap/2017170149
9. Wei, C. C. (2012). Analyses of Material Properties of Nitrided AISI M2 Steel Treated by Plasma Immersion Ion Implantation (PIII) Process. Advanced Science Letters, 12 (1), 148–154. doi: https://doi.org/10.1166/asl.2012.2807
10. Sobol', O. V., Andreev, A. A., Gorban', V. F. (2016). Structural Engineering of Vacuum-ARC Multiperiod Coatings. Metal Science and Heat Treatment, 58 (1-2), 37–39. doi: https://doi.org/10.1007/s11041-016-9961-3
11. Nii, H., Nishimoto, A. (2012). Surface modification of ferritic stainless steel by active screen plasma nitriding. Journal of Physics: Conference Series, 379, 012052. doi: https://doi.org/10.1088/1742-6596/379/1/012052
12. Aydin, H., Bayram, A., Topçu, Ş. (2013). Friction Characteristics of Nitrided Layers on AISI 430 Ferritic Stainless Steel Obtained by Various Nitriding Processes. Materials Science, 19 (1). doi: https://doi.org/10.5755/j01.ms.19.1.3819
13. Araújo, E. de, Bandeira, R. M., Manfrinato, M. D., Moreto, J. A., Borges, R., Vales, S. dos S. et. al. (2019). Effect of ionic plasma nitriding process on the corrosion and micro-abrasive wear behavior of AISI 316L austenitic and AISI 470 super-ferritic stainless steels. Journal of Materials Research and Technology, 8 (2), 2180–2191. doi: https://doi.org/10.1016/j.jmrt.2019.02.006
14. Köster, K., Kaestner, P., Bräuer, G., Hoche, H., Troßmann, T., Oechsner, M. (2013). Material condition tailored to plasma nitriding process for ensuring corrosion and wear resistance of austenitic stainless steel. Surface and Coatings Technology, 228, S615–S618. doi: https://doi.org/10.1016/j.surfcoat.2011.10.059
15. Sobol', O. V., Meilekhov, A. A. (2018). Conditions of Attaining a Superhard State at a Critical Thickness of Nanolayers in Multiperiodic Vacuum-Arc Plasma Deposited Nitride Coatings. Technical Physics Letters, 44 (1), 63–66. doi: https://doi.org/10.1134/s1063785018010224
16. Sun, Y., Chen, Y., Tsuji, N., Guan, S. (2020). Microstructural evolution and mechanical properties of nanostructured Cu/Ni multilayer fabricated by accumulative roll bonding. Journal of Alloys and Compounds, 819, 152956. doi: https://doi.org/10.1016/j.jallcom.2019.152956
17. Nayak, B. K., Elchidana, P., Mohapatra, R., Sahu, P. K. (2016). Optimization of Coating Process by Using Design of Experiment and Thermodynamic Environment Equivalency Factor. Asian Journal of Chemistry, 28 (7), 1589–1594. doi: https://doi.org/10.14233/ajchem.2016.19764
18. Sobol', O. V., Andreev, A. A., Gorban', V. F., Stolbovoy, V. A., Melekhov, A. A., Postelnyk, A. A. (2016). Possibilities of structural engineering in multilayer vacuum-arc ZrN/CrN coatings by varying the nanolayer thickness and application of a bias potential. Technical Physics, 61 (7), 1060–1063. doi: https://doi.org/10.1134/s1063784216070252
19. Byeon, S. S., Wang, K., Seo, Y. J., Jung, Y. G., Koo, B. H. (2012). Structural properties of the oxide coatings prepared by electrolyte plasma process on the Al 2021 alloy in various nitrogen solutions. Ceramics International, 38, S665–S668. doi: https://doi.org/10.1016/j.ceramint.2011.05.131

20. Subbotina, V. V., Sobol, O. V., Belozerov, V. V., Makhatilova, A. I., Shnayder, V. V. (2019). Use of the Method of Micro-arc Plasma Oxidation to Increase the Antifriction Properties of the Titanium Alloy Surface. Journal of Nano- and Electronic Physics, 11 (3), 03025-1–03025-5. doi: https://doi.org/10.21272/jnep.11(3).03025
21. Dunleavy, C. S., Golosnoy, I. O., Curran, J. A., Clyne, T. W. (2009). Characterisation of discharge events during plasma electrolytic oxidation. Surface and Coatings Technology, 203 (22), 3410–3419. doi: https://doi.org/10.1016/j.surfcoat.2009.05.004
22. Dunleavy, C. S., Curran, J. A., Clyne, T. W. (2011). Self-similar scaling of discharge events through PEO coatings on aluminium. Surface and Coatings Technology, 206 (6), 1051–1061. doi: https://doi.org/10.1016/j.surfcoat.2011.07.065
23. Dunleavy, C. S., Curran, J. A., Clyne, T. W. (2013). Time dependent statistics of plasma discharge parameters during bulk AC plasma electrolytic oxidation of aluminium. Applied Surface Science, 268, 397–409. doi: https://doi.org/10.1016/j.apsusc.2012.12.109
24. Nominé, A., Troughton, S. C., Nominé, A. V., Henrion, G., Clyne, T. W. (2015). High speed video evidence for localised discharge cascades during plasma electrolytic oxidation. Surface and Coatings Technology, 269, 125–130. doi: https://doi.org/10.1016/j.surfcoat.2015.01.043
25. Arrabal, R., Matykina, E., Hashimoto, T., Skeldon, P., Thompson, G. E. (2009). Characterization of AC PEO coatings on magnesium alloys. Surface and Coatings Technology, 203 (16), 2207–2220. doi: https://doi.org/10.1016/j.surfcoat.2009.02.011
26. Belozerov, V., Mahatilova, A., Sobol', O., Subbotina, V., Subbotin, A. (2017). Improvement of energy efficiency in the operation of a thermal reactor with submerged combustion apparatus through the cyclic input of energy. Eastern-European Journal of Enterprise Technologies, 2 (5 (86)), 39–43. doi: https://doi.org/10.15587/1729-4061.2017.96721
27. Subbotina, V., Al-Qawabeha, U. F., Belozerov, V., Sobol, O., Subbotin, A., Tabaza, T. A., Al-Qawabah, S. M. (2019). Determination of influence of electrolyte composition and impurities on the content of α-Al_2O_3 phase in MAO-coatings on aluminum. Eastern-European Journal of Enterprise Technologies, 6 (12 (102)), 6–13. doi: https://doi.org/10.15587/1729-4061.2019.185674
28. Yuting, D., Zhiyang, L., Guofeng, M. (2020). The research progress on micro-arc oxidation of aluminum alloy. IOP Conference Series: Materials Science and Engineering, 729, 012055. doi: https://doi.org/10.1088/1757-899x/729/1/012055
29. Durdu, S., Bayramoğlu, S., Demirtaş, A., Usta, M., Üçışık, A. H. (2013). Characterization of AZ31 Mg Alloy coated by plasma electrolytic oxidation. Vacuum, 88, 130–133. doi: https://doi.org/10.1016/j.vacuum.2012.01.009
30. Belozerov, V., Sobol, O., Mahatilova, A., Subbotina, V., Tabaza, T. A., Al-Qawabeha, U. F., Al-Qawabah, S. M. (2018). Effect of electrolysis regimes on the structure and properties of coatings on aluminum alloys formed by anodecathode micro arc oxidation. Eastern-European Journal of Enterprise Technologies, 1 (12 (91)), 43–47. doi: https://doi.org/10.15587/1729-4061.2018.121744
31. Clyne, T. W., Troughton, S. C. (2018). A review of recent work on discharge characteristics during plasma electrolytic oxidation of various metals. International Materials Reviews, 64 (3), 127–162. doi: https://doi.org/10.1080/09506608.2018.1466492
32. Morais, P. J., Gomes, B., Santos, P., Gomes, M., Gradinger, R., Schnall, M. et. al. (2020). Characterisation of a High-Performance Al–Zn–Mg–Cu Alloy Designed for Wire Arc Additive Manufacturing. Materials, 13 (7), 1610. doi: https://doi.org/10.3390/ma13071610
33. Li, J., Li, F., Ma, X., Li, J., Liang, S., Zhang, L. (2018). Effects of Heat Treatment on Microstructure and Mechanical Properties of an ECAPed Al- Zn- Mg- Cu Alloy. Advanced Engineering Materials, 20 (9), 1701155. doi: https://doi.org/10.1002/adem.201701155
34. Stemper, L., Mitas, B., Kremmer, T., Otterbach, S., Uggowitzer, P. J., Pogatscher, S. (2019). Age-hardening of high pressure die casting AlMg alloys with Zn and combined Zn and Cu additions. Materials & Design, 181, 107927. doi: https://doi.org/10.1016/j.matdes.2019.107927
35. Gloria, A., Montanari, R., Richetta, M., Varone, A. (2019). Alloys for Aeronautic Applications: State of the Art and Perspectives. Metals, 9 (6), 662. doi: https://doi.org/10.3390/met9060662
36. Fridlyander, I. N. (2004). Alyuminievye splavy v aviaraketnoy i yadernoy tehnike. Vestnik Rossiyskoy Akademii Nauk, 74 (12), 1076–1081.
37. Dos Santos, J. F., Staron, P., Fischer, T., Robson, J. D., Kostka, A., Colegrove, P. et. al. (2018). Understanding precipitate evolution during friction stir welding of Al-Zn-Mg-Cu alloy through in-situ measurement coupled with simulation. Acta Materialia, 148, 163–172. doi: https://doi.org/10.1016/j.actamat.2018.01.020
38. Suminov, I. V., Epel'fel'd, A. V., Lyudin, V. B., Borisov, A. M., Krit, B. L. (2001). Mikrodugovoe oksidirovanie (obzor). Pribory, 9, 13–23.
39. Subbotina, V., Sobol, O., Belozerov, V., Al-Qawabeha, U. F., Tabaza, T. A., Al-Qawabah, S. M., Shnayder, V. (2020). A study of the electrolyte composition influence on the structure and properties of MAO coatings formed on AMg_6 alloy. Eastern-European Journal of Enterprise Technologies, 3 (12 (105)), 6–14. doi: https://doi.org/10.15587/1729-4061.2020.205474
40. Subbotina, V. V., Al-Qawabeha, U. F., Sobol', O. V., Belozerov, V. V., Schneider, V. V., Tabaza, T. A., Al-Qawabah, S. M. (2019). Increase of the α-Al_2O_3 phase content in MAO-coating by optimizing the composition of oxidated aluminum alloy. Functional Materials, 26 (4), 752–758. doi: https://doi.org/10.15407/fm26.04.752
41. Sobol', O. V., Shovkoplyas, O. A. (2013). On advantages of X-ray schemes with orthogonal diffraction vectors for studying the structural state of ion-plasma coatings. Technical Physics Letters, 39 (6), 536–539. doi: https://doi.org/10.1134/s1063785013060126
42. Klopotov, A. A., Abzaev, Yu. A., Potekaev, A. I., Volokitin, O. G. (2012). Osnovy rentgenostrukturnogo analiza v materialovedenii. Tomsk: Izd-vo TGASU, 275.
43. Suminov, I. V., Belkin, P. N., Epel'fel'd, A. V., Lyudin, V. B., Krit, B. L., Borisov, A. M. (2011). Plazmenno-elektroliticheskoe modifitsirovanie poverhnosti metallov i splavov. Vol. 2. Moscow: Tehnosfera, 512.
44. Loyola, C., Menéndez-Proupin, E., Gutiérrez, G. (2010). Atomistic study of vibrational properties of γ-Al_2O_3. Journal of Materials Science, 45 (18), 5094–5100. doi: https://doi.org/10.1007/s10853-010-4477-5
45. Prins, R. (2019). Positionen von Spinellfehlstellen in γ-Al_2O_3. Angewandte Chemie, 131 (43), 15694–15698. doi: https://doi.org/10.1002/ange.201901497